Microbial Ecology

Heterotrophic Pioneers Facilitate Phototrophic Biofilm Development

G. Roeselers, M. C. M. van Loosdrecht and G. Muyzer

Department of Biotechnology, Delft University of Technology, Julianalaan 67, NL-2628 BC Delft, The Netherlands

Received: 5 December 2006 / Accepted: 26 February 2007 / Online publication: 18 March 2007

Abstract

Phototrophic biofilms are matrix-enclosed microbial communities, mainly driven by light energy. In this study, the successional changes in community composition of freshwater phototrophic biofilms growing on polycarbonate slides under different light intensities were investigated. The sequential changes in community composition during different developmental stages were examined by denaturing gradient gel electrophoresis (DGGE) of polymerase chain reaction (PCR)-amplified 16S rRNA gene fragments in conjugation with sequencing and phylogenetic analysis. Biofilm development was monitored with subsurface light sensors. The development of these biofilms was clearly light dependent. It was shown that under high light conditions the initial colonizers of the substratum predominantly consisted of green algae, whereas at low light intensities, heterotrophic bacteria were the initial colonizers. Cluster analysis of DGGE banding patterns revealed a clear correlation in the community structure with the developmental phases of the biofilms. At all light intensities, filamentous cyanobacteria affiliated to *Microcoleus vaginatus* became dominant as the biofilms matured. It was shown that the initial colonization phase of the phototrophic biofilms is shorter on polycarbonate surfaces precolonized by heterotrophic bacteria.

Introduction

Phototrophic biofilms are formed on surfaces in a range of terrestrial and aquatic environments (e.g., [7, 15, 20]). The major energy source in these biofilms is photosynthesis. Aerobic diatoms, green algae, and cyanobacteria use light energy and reduce carbon dioxide, providing organic substrates and oxygen. The photosynthetic activity fuels processes in the total biofilm community, including the heterotrophic fraction [6, 21]. The microorganisms produce extracellular polymeric substances (EPS) that hold the biofilm together [8, 23].

There is a growing interest in the application of phototrophic biofilms, for instance in wastewater treatment in constructed wetlands, bioremediation [26, 30], aquaculture [3], and in the development of antifouling agents [4, 5, 22]. To be able to optimize biofilm development for specific applications it is key to understand the structure and functioning of phototrophic biofilms. The laboratory-based cultivation of phototrophic biofilms provides a valuable alternative for natural systems by allowing experimental manipulation of the entire microbial ecosystem.

In this study, we addressed the formation of oxygenic phototrophic biofilms in the context of primary ecological succession. Successional community changes during the colonization of new habitats or after environmental disturbances have been described for communities of planktonic and benthic microalgae [12, 24], and more recently in bacterial communities [9, 14, 18]. Primary succesional development of an ecosystem is always initiated by the settlement of pioneer organisms in a previously uncolonized environment. In the present work, we have studied the early events of surface colonization to identify pioneer organisms that initiate phototrophic biofilm succession.

We cultivated biofilms in a specially developed flow-lane incubator with controlled external light, temperature, and flow velocity. In addition, cultivation experiments were carried out in small flow-cell-type incubators. The growth of the biofilms was monitored continuously. DGGE of PCR-amplified SSU rRNA gene fragments in conjunction with Unweighted Pair Group Method with Arithmetic mean (UPGMA) clustering analysis, DNA

Correspondence to: G. Muyzer; E-mail: g.muijzer@tudelft.nl

 DOI: 10.1007/s00248-007-9238-x • Volume 54, 578–585 (2007)

sequencing and phylogenetic analysis were used to monitor changes in the community composition of the biofilms that developed under different light conditions.

Materials and Methods

Biofilm incubator. The incubator used in this study contained four separate flow channels through which a volume of 4 L medium circulated over a surface covered with 47 polycarbonate slides ($76 \times 25 \times 1$ mm). Polycarbonate slides were used as a substratum for biofilm adhesion. Each light chamber contained an adjustable light source and the circulation speed of the culture medium could be regulated precisely. The medium was refreshed twice a week. Biofilm growth was monitored and recorded with three light sensors that were positioned directly under selected polycarbonate slides. Each light sensor contained three independent photodiodes. Light absorbance was used as an indicator for biomass accumulation. The incubator design was described in more detail by Zippel & Neu [33].

In addition, aluminum flow-cell type incubators with a channel dimension of $4 \times 26 \times 108$ mm, covered with polycarbonate lids were used. The aluminum body of the flow cells contained a water channel for temperature control. The transparent polycarbonate lids formed the substratum for biofilm growth.

Growth conditions and inoculum. The mineral medium used was a modification of the BG11 as described by Stanier et al. [28]. Ammonium ferric citrate green was replaced by FeCl3. The vitamins cyanocobalamin (40 μg/L), thiamine HCL (40 μg/L), and biotin (40 μg/L) were added. $NaSiO_3 \cdot 9H_20$ (57 mg/mL) was added to allow the growth of freshwater diatoms.

Phototrophic biofilm samples obtained from a sedimentation tank of the wastewater treatment plant (WWTP) at Fiumicino Airport (Rome, Italy) were used as inoculum of biofilm development at the polycarbonate slides within the flow lane incubator. The community composition of these environmental phototrophic biofilms was described in detail by Albertano et al. [1]. To reduce predation pressure, inocula were frozen for 2 days at −20°C to kill protozoa, metazoa, and nematodes.

The biofilms were grown at 20°C and at a medium flow rate of 100 L/h. The biofilms were grown under a photon flux density (PFD) of 15, 30, 60, and 120 μmol photons m^{-2} s^{-1}. A diurnal cycle of 16 h light and 8 h dark was applied. The growth and development of the biofilms was monitored for 35 days.

The influence of heterotrophic bacteria on the development of phototrophic biofilms was studied in separate biofilm cultivation experiments. Two identical flow cells were inoculated with an environmental phototrophic biofilm sample collected from a helophyte pond system from the municipal WWTP at St. Maartensdijk (The Netherlands) and incubated for 7 days in complete darkness. Flow cells with modified BG11 medium were maintained at a constant temperature of 20°C, an irradiance of 60 μmol photons m^{-2} s^{-1}, and a flow rate of 0.5 L/h.

After 7 days the transparent polycarbonate top of one flow cell (flow cell II) was replaced by a new sterile top. Both flow cells were again inoculated and biofilm development on the polycarbonate top lid was documented over a period of 20 days.

Image analysis of biofilm scans. A CanoScan LiDE 60 flatbed scanner (Cannon Inc., Tokyo, Japan) was used to capture images of the polycarbonate incubated in the flow cells (I and II). Every day, the lids were removed from the flow cells and gently placed on the glass surface of the flatbed scanner. Slides were covered with a white plastic tray to exclude external light. The resulting scans were saved as an 8-bit tagged image file format (TIFF). Image analysis was performed using ImageJ 1.36b (National Institutes of Health [NIH], Bethesda, MD, USA). Lids were carefully placed back onto the flow cells for further incubation. Mean and standard deviation of the gray values of each image were calculated using the integrated measurement tool. It must be noted that the tone value of an 8-bit pixel ranges from 0 to 255, where 0 is the blackest black and 255 is the whitest white.

Sample collection. Biofilms grown under four different light conditions were sampled when they reached the initial colonization, exponential, and mature phase of their development. These phases were defined as the times when the subsurface light sensors measured, 10, 50, and 80% light absorbance, respectively. One polycarbonate slide was removed from the incubator lanes at the exit side of the flow lane at each sampling event. The samples were immediately stored at −20°C for further analysis. Duplicate samples were examined by bright-field microscopy (×100 to ×400 magnification) with a Zeiss Axioplan microscope (Carl Zeiss, Jena, Germany).

DNA extraction. Biofilm biomass was scraped from the slides with a sterile razorblade. Genomic DNA was extracted by applying approximately 300 mg biomass to the UltraClean Soil DNA Isolation Kit TM (Mo Bio Laboratories, Carlsbad, CA, USA) according to the manufacturer's protocol. Complete cell lysis was verified afterward by using phase-contrast microscopy. The quantity and quality of the extracted DNA were analyzed by spectrophotometry using the NanoDrop ND-1000 TM (NanoDrop Technologies, Wilmington, DE, USA) and by agarose gel electrophoresis. DNA dilutions were stored at −20°C.

Polymerase chain reaction (PCR) amplification of rRNA gene fragments. Extreme care was taken to prevent any DNA contamination of solutions and plastic disposables used for PCR. All heat sterilized plastic tubes were exposed to UV light for 30 min before use. Only DNA- and RNA-free water (W4502, Sigma-Aldrich, St. Louis, MO, USA) was used to prepare PCR reagent stock solutions and PCR reaction mixtures.

To amplify the bacterial 16S rRNA encoding gene fragments, the DNA dilutions were used as template DNA in 50-µl PCR reactions using the primers 341F-GC and 907R, and PCR conditions as described by Schäfer et al. [24]. This PCR was carried out with a denaturation step of 5 min at 94°C, followed by 35 cycles of denaturation of 1 min at 94°C, annealing of 1 min at 60°C, and extension of 1 min at 72°C, followed by a final extension step of 15 min at 72°C. All amplification reactions were performed in a T1 Thermocycler (Biometra, Westburg, the Netherlands).

Denaturing gradient gel electrophoresis of Polymerase chain reaction (PCR) products. Denaturing gradient gel electrophoresis (DGGE) was performed as described by Schäfer & Muyzer [25]. Briefly, 1-mm thick 6% acrylamide gels with a urea–formamide gradient of 20–80% were used for bacterial 16S rRNA gene fragments. Gels were run in Tris–acetate–EDTA buffer for 16 h at 100 V and at a constant temperature of 60°C. Gels were stained in an ethidium bromide solution and analyzed and photographed using the GelDoc UV Transilluminator (BioRad, Hercules, CA, USA).

The dominant bands were excised from the DGGE gels with a sterile surgical scalpel. Each small gel slice was placed in 15 µl of sterile water for 24 h at 4°C. Subsequently, 2 µl of the solution was used as template DNA for reamplification as described above. The PCR products were again subjected to DGGE analysis to confirm the purity and their position relative to the bands from which they were originally excised. The PCR products were purified using the QIAquick Gel Extraction Kit (QIAGEN, Hilden, Germany). Purified PCR products were sequenced by a commercial company (BaseClear, Leiden, the Netherlands). DGGE profiles were compared visually on the basis of the presence and relative density of bands. In addition, the presence and absence of DGGE bands in different samples were scored in binary matrices. This binary matrix was translated into a distance matrix using the Jaccard coefficient. A dendrogram was then constructed by the UPGMA clustering method [11]. Jaccard coefficient and UPGMA calculations were done with the software package Primer 6 (PRIMER-E Ltd, Plymouth, UK).

Comparative sequence analysis. Partial 16S rRNA gene sequences with a length between 400 and 500 bp were first compared to the sequences stored in the GenBank nucleotide database using the BLAST algorithm [2] to obtain a first identification of the biofilm community members. Subsequently, the sequences were imported into the ARB SSU rRNA database (available at http://www.arb-home.de) [17]. The dissimilarity values were used to calculate distance matrixes. Distance matrix trees were generated by the Neighbor-Joining (NJ) method with the Felsenstein correction as implemented in the PAUP 4.0B software (Sinauer, Sunderland, MA, USA). The NJ calculation was subjected to bootstrap analysis (1000 replicates).

The DNA sequences obtained in this study were deposited in the GenBank Nucleotide database and assigned accession numbers DQ388949 to DQ388967.

Results

Biofilm development. Biofilm growth was monitored by the decrease of subsurface light. The duration of the initial colonization phase after inoculation was ~8 days in the biofilms grown at a photon flux density (PFD) of 60 and 120 µmol photons m^{-2} s^{-1} (Fig. 1). At 30-µmol photons m^{-2} s^{-1}, the initial phase lasted until ~22 days after inoculation. The biofilm growing at 15-µmol photons m^{-2} s^{-1} did not show an exponential growth phase. Therefore, the second and third PFD 15 samples were collected at day 25 and day 35, respectively. The fluctuations in light absorbance after higher light biofilms reached their mature phase were caused by detachment and subsequent recolonization of parts of the biofilm, also known as sloughing [29].

The average dry weight per slide at the end of the growth experiment was approximately 0.15 g in the PFD 60 and PFD 120 lanes, about 0.06 g in the PFD 30 lane and 0.008 g in the PFD 15 lane. This shows that the sensors are suitable for monitoring biomass increase, but they are not suitable as indicators for the actual biomass.

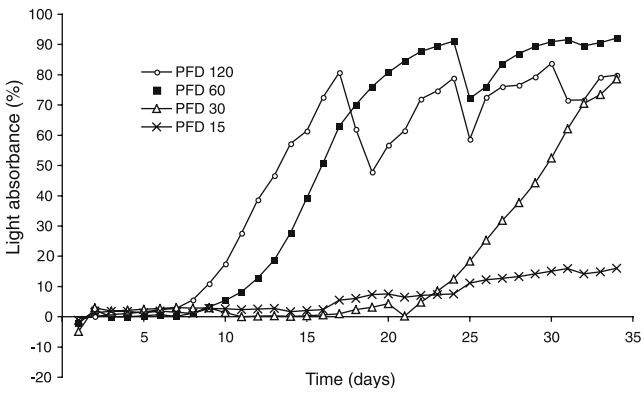

Figure 1. Growth curves of phototrophic biofilms growing at four incident light intensities (120, 60, 30, and 15 µmol photons m^{-2} s^{-1}). Biofilm development is indicated as the increasing light absorbance derived from the decrease of subsurface light.

Molecular analysis of the microbial community. The DGGE band patterns describing bacterial community diversity during the initial, exponential, and mature phases of biofilm development under the four different light intensities were all different. The initial phase DGGE patterns from the high light intensity biofilms (PFD 60 and 120) shared two dominant bands (Fig. 2, bands 1 and 4). Band 1 was affiliated to the chloroplast of *Scenedesmus obliquus* and band 4 was affiliated to an unidentified member of the Bacteroidetes (formerly known as the Cytophaga-Flavobacteria-Bacteroides (CFB) group). The presence of *Scenedesmus*-like unicellular algae in the initial phase at high light intensity was confirmed by microscopic observations. Bands at the same position in the gel and with the same phylogenetic affiliation as band 1 were also present during the exponential and mature phase at high light intensities. During the exponential phase, thick dominant bands appeared at similar positions in the DGGE profiles of the PFD 60 and PFD 120 biofilms. These bands represented DNA sequences affiliated to the filamentous cyanobacterium *Microcoleus vaginatus*, a known inhabitant of desert soil crusts [10] (Fig. 2, bands 8, 12, 13, and 17, and Fig. 3). However, the bands corresponding to *Scenedesmus obliquus* were also present during the mature phase. Light microscopic observations confirmed that during the exponential and mature phase, the top layer of the biofilm consisted predominantly of *Microcoleus* filaments, which covered the *Scenedesmus*-like cells.

The initial colonization phase of the lower light intensity biofilms (15 and 30 μmol) was characterized by the presence of one dominant band affiliated to the β-proteobacteria. The exponential phase DGGE pattern of the PFD 30 biofilm showed three dominant bands corresponding to *Scenedesmus obliquus, Microcoleus vaginatus*, and *Synechocystis* sp. The pattern from the mature phase PFD 30 samples showed two dominant bands corresponding to sequences affiliated to *Microcoleus vaginatus* and *Synechocystis* sp. (Fig. 2, bands 16 and 17). The *Scenedesmus obliquus* band had almost completely disappeared. After 35 days, the PFD 15 biofilms showed bands affiliated to unicellular *Synechocystis*-like cyanobacteria. (Fig. 2, band 19, and Fig. 3). The presence of unicellular cyanobacteria was confirmed by light microscopy.

The UPGMA dendogram (Fig. 4) constructed from the DGGE profiles shows the highest similarity between samples from similar developmental phases. It is remarkable that the dendogram shows one big cluster with the initial phase DGGE patterns and one cluster with the exponential and mature phase DGGE patterns. However, DGGE patterns from the three PFD 15 biofilm samples were all in one cluster.

Role of heterotrophic pioneers. To get a better understanding of the role of heterotrophs in the phototrophic biofilm, a separate cultivation experiment was conducted using small flow cells. Analysis of surface images obtained with the scanner showed that the more biomass developed on the flow-cell lid the darker the image would appear. Although the actual biomass was not determined, we assumed that

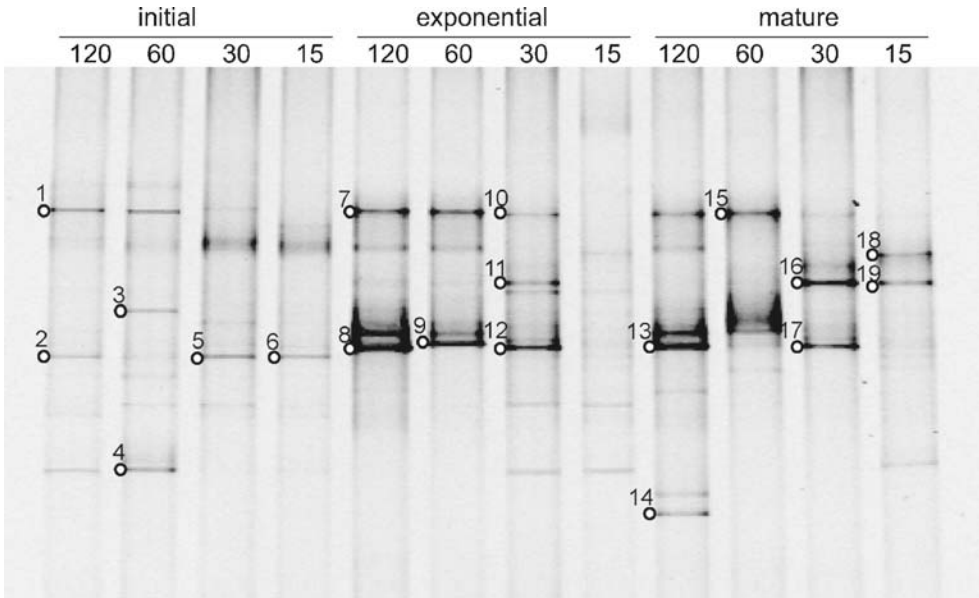

Figure 2. DGGE patterns of 16S rRNA gene fragments obtained after enzymatic amplification using general bacterial primers and genomic DNA samples from phototrophic biofilms growing at four incident light intensities (120, 60, 30, and 15 μmol photons m^{-2} s^{-1}). Samples were collected during the initial, exponential, and mature phases of biofilm development. Numbers at the left of each lane correspond to bands that were excised, PCR amplified, and sequenced.

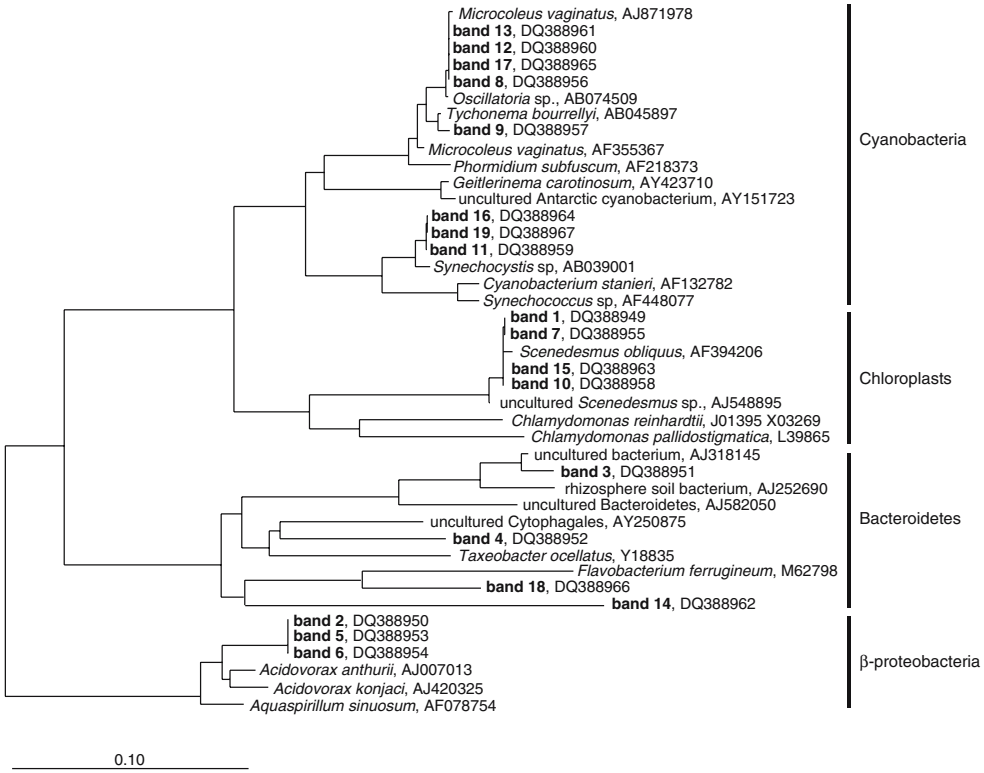

Figure 3. Evolutionary tree showing the phylogenetic affiliations as revealed by comparative analysis of the general bacterial 16S rRNA gene sequences derived from the DGGE bands shown in Fig. 2. The sequences obtained in this study are printed bold. *Escherichia coli* (AJ567606) was used as an out-group, but was pruned from the tree. Bootstrap values based on 1000 replicates are indicated for branches supported by >50% of trees. Scale bar indicates 10% estimated sequence divergence.

changing average gray values could be used as an indirect indication of biofilm growth. A similar biofilm analysis method was applied by Milferstedt et al. [19]. In this study, it was shown that average biofilm biomass is highly correlated with the gray levels of biofilm images obtained with a scanner.

Biofilm growth on polycarbonate surface preincubated in the dark was compared with that on pristine polycarbonate surface. Mean gray values calculated for each slide scan showed that the duration of the initial colonization phase on the slides that were preincubated in the dark was shorter than on new sterile slides (Fig. 5A

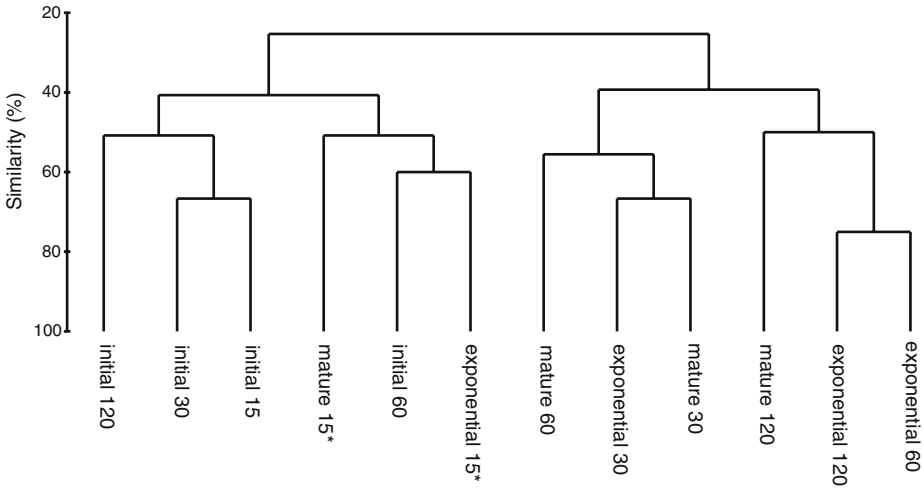

Figure 4. UPGMA dendogram showing the combined clustering analyses of digitized DGGE profiles (Fig. 2). The analysis is based on the presence or absence of bands at certain positions in each lane of the gel. *The biofilm cultivated at 15 μmol photons m^{-2} s^{-1} did not reach 50 and 80% light absorbance.

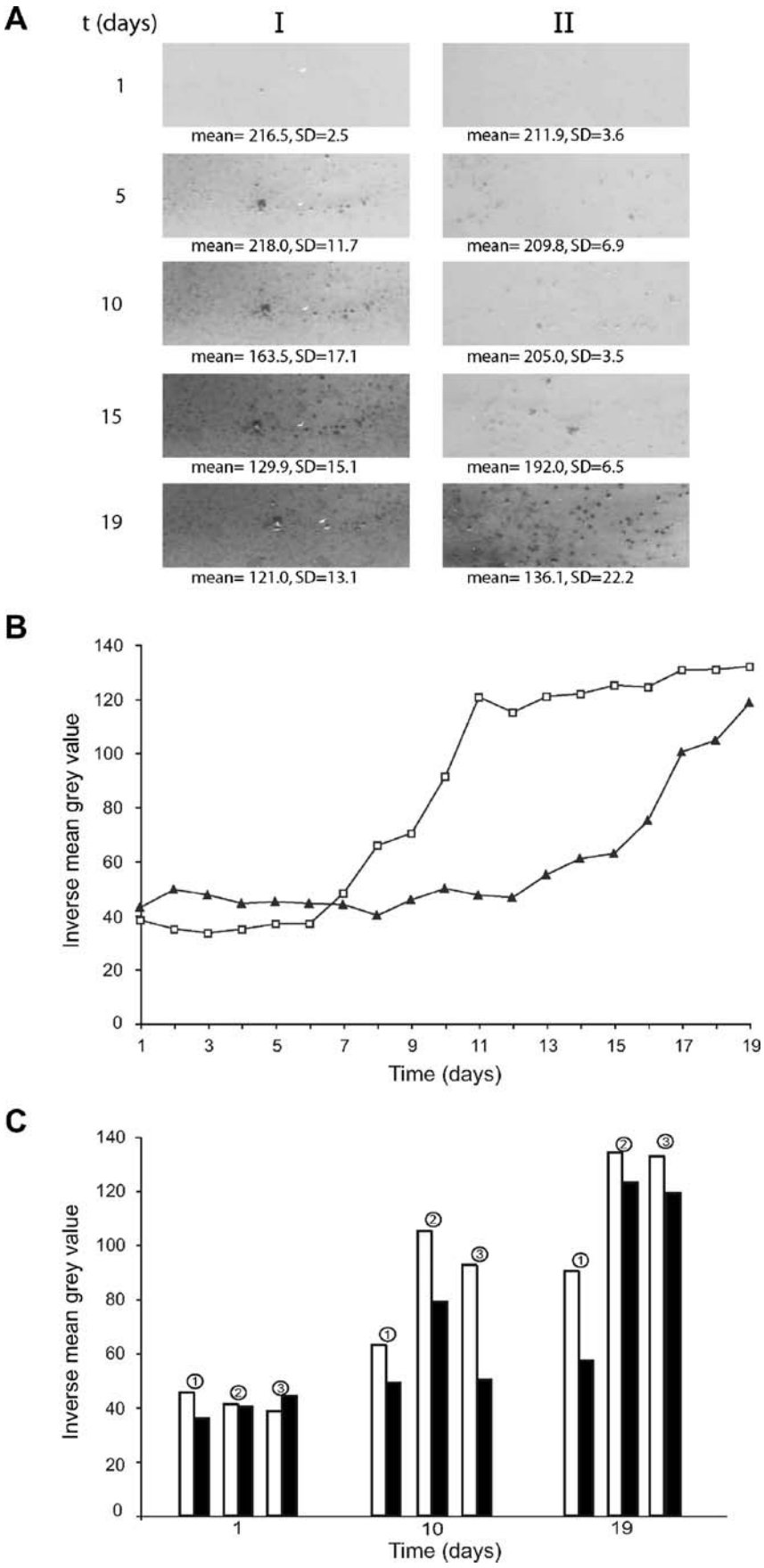

Figure 5. Biofilm development on polycarbonate incubated in two flow cells. Both flow cells were preincubated for 7 days with inoculated BG11 medium in complete darkness. At day 8, the polycarbonate lid of flow cell II was changed. Subsequently, both flow cells were subjected to 60 μmol photons m^{-2} s^{-1} irradiation for 19 days. (**A**) Column I (flow cell I) and II (flow cell II) show images of the lids that were scanned at different time points. The mean and standard deviation (SD) of the pixel gray values in the scanned area are indicated under each image. It must be noted that the gray value of an 8-bit pixel ranges from 0 to 255. (**B**) Inverse of the mean gray values of biofilm images captured over a period of 19 days: (□) Flow-cell I, (▲) Flow-cell II. (**C**) Replicate experiments showing biofilm development on precolonized polycarbonate (Flow cell I, white) and pristine polycarbonate (Flow cell II, black) after 1, 10, and 19 days of incubation. Replicates are indicated as 1, 2, and 3.

and B). Replicate experiments showed the same trend, although the rate at which biofilms developed was variable (Fig. 5C). Microscopic examination confirmed that after 7 days of preincubation in the dark, the polycarbonate lids were colonized by heterotrophic bacteria.

Discussion

Our results show that the cultivated biofilms were inhabited by a phylogenetically diverse array of microorganisms. We found sequences affiliated to eukaryote chloroplasts, cyanobacteria, β-proteobacteria, and the Bacteroidetes group. The community composition of the cultivated phototrophic biofilms clearly changed over time.

The daily increase in light absorbance during the exponential phase was similar for the light intensities of 30, 60, and 120 μmol photons m^{-2} s^{-1}. We only observed that the duration of the initial colonization phase increased when light intensities decreased. We think that cyanobacteria are responsible for the exponential growth of the biofilm because we observed dominant DGGE bands representing filamentous cyanobacterial species in the profiles of the exponential and mature phase biofilms. The UPGMA analysis of the DGGE patterns shows one cluster with the initial phase biofilms and one cluster with the exponential and mature phase biofilms. This indicates that these biofilm communities experienced similar changes in biodiversity during their development. The fact that the DGGE patterns from the three developmental phases of the low-light biofilm (PFD 15) clustered together in the UPGMA dendogram suggests that the low-light biofilm did not really mature during the experimental time.

The phylogenetic analysis of DGGE bands showed that at high light intensities unicellular algae affiliated to *Scenedesmus* sp. attached first to the polycarbonate substratum. It seems that as soon as the surface was covered with some biomass, *Microcoleus vaginatus* strains were able to overgrow the biofilm resulting in an exponential increase in biofilm thickness. At lower light intensities, the polycarbonate surface was initially colonized by β-proteobacteria. Previous studies showed that heterotrophic bacteria play an important role as early colonizers during biofilm development on submerged glass slides in a marine environment [7].

The exponential growth of the PFD 30 biofilm was also caused by the rapid growth of *M. vaginatus*-like cyanobacteria. However, the exponential and mature stages of the PFD 15 and PFD 30 biofilms also contained unicellular *Synechocystis*-like cyanobacteria. It could be hypothesized that filamentous cyanobacteria outcompete unicellular cyanobacteria for light by their ability to migrate toward optimal light conditions. At lower light intensities this advantage could be reduced because of a lower light-affinity coefficient [27, 31].

It is possible that the succession observed in the large flow lane incubator mainly occurred because conditions in the biofilm changed, largely because of microbial activity and growth itself. Early colonizers might change the environmental conditions in the biofilm, e.g., by altering the substratum surface [16, 18], and hence facilitating the attachment of filamentous cyanobacteria.

Another explanation for the dominance of cyanobacteria in the exponential and mature phase biofilms could be the different critical light intensities of algae and cyanobacteria [32]. The initially fast growing *Scenedesmus* strains may experience increasing light limitation resulting from self-shading. Although cyanobacteria cannot reach the maximum growth rates of green algae, they show higher growth rates at low light intensities. Competition experiments in light-limited chemostats with cultures of *Aphanizomenon*, *Microcystis*, and *Scenedesmus* sp. by Huisman et al. [13] showed that the cyanobacteria outcompete *Scenedesmus* for light, independent of their initial abundance. This critical light intensity effect has not been described before for benthic communities. An important difference between continuous suspended cultures and cultivated biofilms is that the dilution rate of the reactor imposes no artificial loss factor on biofilm communities.

Our separate cultivation experiments with the flow cells seem to confirm the importance of heterotrophic pioneers [7]. Analysis of the polycarbonate surface scans suggests that colonization by heterotrophic bacteria enhances the establishment of a phototrophic biofilm. However, it is also possible that the observed difference in biofilm growth is a result of surface conditioning by the association of organic compounds to the polycarbonate.

Because the mineral medium used in the incubator contained no organic carbon, it seems that heterotrophic pioneers utilized organic compounds that were present in the inoculum. The slow growth of heterotrophs at relatively low carbon conditions could explain the long initial phase at low light intensities. It is possible that at higher light intensities phototrophic pioneers like *Scenedesmus* sp. grow faster and provide the system with sufficient carbon.

In conclusion, our results show that the development of phototrophic biofilms under controlled conditions involves a series of successional community changes. The influence of light on the biofilm growth rate and the community composition appeared more prevalent during the initial phase of biofilm development. Phototrophic biofilms developed faster on polycarbonate surfaces that were precolonized by heterotrophic bacteria.

These data illustrate that although a mature biofilm community can be dominated by a few species, there is also a minor set of organisms, e.g., heterotrophic bacteria, that may be crucial for the initial establishment and the consequent development of that biofilm com-

munity. These results may have implications for the cultivation of phototrophic biofilms in wastewater treatment applications and for control of biofouling dominated by phototrophic biofilms. Future experiments should focus on the mechanisms by which heterotrophic precolonization enhances phototrophic biofilm development.

Acknowledgements

This research was supported by the European Union (PHOBIA project, contract QLK3-CT-2002-01938). We thank Marc Staal (NIOO-KNAW Centre for Estuarine and Marine Ecology, the Netherlands) for the design of the flow-cell incubator. We thank our coworkers in the Environmental Biotechnology group for careful reading and commenting on the manuscript.

References

1. Albertano, P, Congestri, R, Shubert, LE (1999) Cyanobacterial biofilms in sewage treatment plants along the Thyrrenian coast (Mediterranean Sea), Italy. Arch Hydrobiol Suppl Algol Stud 94: 13–24
2. Altschul, SF, Gish, W, Miller, W, Myers, EW, Lipman, DJ (1990) Basic local alignment search tool. J Mol Biol 215: 403–410
3. Bender, J, Phillips, P (2004) Microbial mats for multiple applications in aquaculture and bioremediation. Bioresour Technol 94: 229–238
4. Bhadury, P, Wright, PC (2004) Exploitation of marine algae: biogenic compounds for potential antifouling applications. Planta 219: 561–578
5. Callow, ME, Callow, JE (2002) Marine biofouling: a sticky problem. Biologist (Lond) 49: 10–14
6. Canfield, DE, Des Marais, DJ (1993) Biogeochemical cycles of carbon, sulfur, and free oxygen in a microbial mat. Geochim Cosmochim Acta 57: 3971–3984
7. Chan, BK, Chan, WK, Walker, G (2003) Patterns of biofilm succession on a sheltered rocky shore in Hong Kong. Biofouling 19: 371–380
8. de Brouwer, JF, Wolfstein, K, Ruddy, GK, Jones, TE, Stal, LJ (2005) Biogenic stabilization of intertidal sediments: the importance of extracellular polymeric substances produced by benthic diatoms. Microb Ecol 49: 501–512
9. Ferris, MJ, Nold, SC, Revsbech, NP, Ward, DM (1997) Population structure and physiological changes within a hot spring microbial mat community following disturbance. Appl Environ Microbiol 63: 1367–1374
10. Garcia-Pichel, F, Lopez-Cortes, A, Nübel, U (2001) Phylogenetic and morphological diversity of cyanobacteria in soil desert crusts from the Colorado plateau. Appl Environ Microbiol 67: 1902–1910
11. Griffiths, RI, Whiteley, AS, O'Donnell, AG, Bailey, MJ (2000) Rapid method for coextraction of DNA and RNA from natural environments for analysis of ribosomal DNA- and rRNA-based microbial community composition. Appl Environ Microbiol 66: 5488–5491
12. Helbling, EW, Barbieri, ES, Marcoval, MA, Goncalves, RJ, Villafane, VE (2005) Impact of solar ultraviolet radiation on marine phytoplankton of Patagonia, Argentina. Photochem Photobiol 81: 807–818
13. Huisman, J, Jonker, RR, Zonneveld, C, Weissing, FJ (1999) Competition for light between phytoplankton species: experimental tests of mechanistic theory. Ecology 80: 211–222
14. Jackson, CR (2003) Changes in community properties during microbial succession. Oikos 101: 444–448
15. Jarvi, HP, Neal, C, Warwick, A, White, J, Neal, M, Wickham, HD, Hill, LK, Andrews, MC (2002) Phosphorus uptake into algal biofilms in a lowland chalk river. Sci Total Environ 282–283: 353–373
16. Li, J, Helmerhorst, EJ, Leone, CW, Troxler, RF, Yaskell, T, Haffajee, AD, Socransky, SS, Oppenheim, FG (2004) Identification of early microbial colonizers in human dental biofilm. J Appl Microbiol 97: 1311–1318
17. Ludwig, W, Strunk, O, Westram, R, Richter, L, Meier, H, Kumar, Y, Buchner, A, Lai, T, Steppi, S, Jobb, G, Forster, W, Brettske, I, Gerber, S, Ginhart, AW, Gross, O, Grumann, S, Hermann, S, Jost, R, Konig, A, Liss, T, Lussmann, R, May, M, Nonhoff, B, Reichel, B, Strehlow, R, Stamatakis, A, Stuckmann, N, Vilbig, A, Lenke, M, Ludwig, T, Bode, A, Schleifer, KH (2004) ARB: a software environment for sequence data. Nucleic Acids Res 32: 1363–1371
18. Martiny, AC, Jorgensen, TM, Albrechtsen, HJ, Arvin, E, Molin, S (2003) Long-term succession of structure and diversity of a biofilm formed in a model drinking water distribution system. Appl Environ Microbiol 69: 6899–6907
19. Milferstedt, K, Pons, MN, Morgenroth, E (2006) Optical method for long-term and large-scale monitoring of spatial biofilm development. Biotechnol Bioeng 94: 773–782
20. Ortega-Morales, O, Guezennec, J, Hernandez-Duque, G, Gaylarde, CC, Gaylarde, PM (2000) Phototrophic biofilms on ancient Mayan buildings in Yucatan, Mexico. Curr Microbiol 40: 81–85
21. Paerl, HW, Pinckney, JL, Steppe, TF (2000) Cyanobacterial–bacterial mat consortia: examining the functional unit of microbial survival and growth in extreme environments. Environ Microbiol 2: 11–26
22. Patil, JS, Anil, AC (2005) Biofilm diatom community structure: influence of temporal and substratum variability. Biofouling 21: 189–206
23. Richert, L, Golubic, S, Guedes, RL, Ratiskol, J, Payri, C, Guezennec, J (2005) Characterization of exopolysaccharides produced by cyanobacteria isolated from Polynesian microbial mats. Curr Microbiol 51: 379–384
24. Schäfer, H, Bernard, L, Courties, C, Lebaron, P, Servais, P, Pukall, R, Stackebrandt, E, Troussellier, M, Guindulain, T, Vives-Rego, J, Muyzer, G (2001) Microbial community dynamics in Mediterranean nutrient-enriched seawater mesocosms: changes in the genetic diversity of bacterial populations. FEMS Microbiol Ecol 34: 243–253
25. Schäfer, H, Muyzer, G (2001) Denaturing gradient gel electrophoresis in marine microbial ecology. In: Paul JH (ed.) Methods in Microbiology, Marine Microbiology. Academic Press, New York (Methods in Microbiology, vol 30, pp 425–468
26. Schumacher, G, Blume, T, Sekoulov, I (2003) Bacteria reduction and nutrient removal in small wastewater treatment plants by an algal biofilm. Water Sci Technol 47: 195–202
27. Staal, M, te Lintel Hekkert, S, Herman, P, Stal, LJ (2002) Comparison of models describing light dependence of N2 fixation in heterocystous cyanobacteria. Appl Environ Microbiol 68: 4679–4683
28. Stanier, RY, Kunisawa, R, Mandel, M, Cohen-Bazire, G (1971) Purification and properties of unicellular blue-green algae (order Chroococcales). Bacteriol Rev 35: 171–205
29. van Loosdrecht, MCM, Eikelboom, D, Gjaltema, A, Mulder, A, Tijhuis, L, Heijnen, JJ (1995) Biofilm structures. Water Sci Technol 32: 35–43
30. Vymazal, J, Sladedek, V, Stach, J (2001) Biota participating in wastewater treatment in a horizontal flow constructed wetland. Water Sci Technol 44: 211–214
31. Walsby, AE (2005) Stratification by cyanobacteria in lakes: a dynamic buoyancy model indicates size limitations met by *Planktothrix rubescens* filaments. New Phytol 168: 365–376
32. Weissing, FJ, Huisman, J (1994) Growth and competition in a light gradient. J Theor Biol 168: 323–336
33. Zippel, B, Neu, TR (2005) Growth and structure of phototrophic biofilms under controlled light conditions. Water Sci Technol 52: 203–209